Submitted to: *International Conference on Pattern Recognition, 1994.*
MIT Media Laboratory Perceptual Computing Group Technical Report #264

Restoration and Enhancement of Fingerprint Images Using M-Lattice – a Novel Non-Linear Dynamical System

Alex Sherstinsky[†‡]
Rosalind W. Picard[‡]

Massachusetts Institute of Technology

[†]Department of Electrical Engineering and Computer Science
[‡]The Media Laboratory

February, 1994

Abstract

In this paper we develop a method for the simultaneous restoration and halftoning of scanned fingerprint images using a novel non-linear dynamical system, called the "M-lattice system". This system is rooted in the reaction-diffusion model, first proposed by Turing in 1952 to explain the formation of animal patterns such as zebra stripes and leopard spots. A typical reaction-diffusion system is a set of heat equations, coupled by non-linear reaction terms. The new M-lattice system is closely related to the analog Hopfield network and the cellular neural network, but has more flexibility in how its variables interact. Furthermore, the state variables of an M-lattice system are guaranteed to be bounded, which is not the case with many reaction-diffusion systems. Due to this large-signal boundedness, the M-lattice system possesses desirable numerical properties that make it useful in engineering applications. Our new method for enhancing fingerprints explores the ability of the M-lattice system to form oriented spatial patterns (like reaction-diffusion systems), while producing binary outputs (like analog feedback neural networks). We compare the outputs of two approaches used to enhance the same original fingerprint: the new M-lattice system and adaptive thresholding, a common halftoning method employed in traditional fingerprint classification systems. The results indicate that the fingerprints synthesized by the M-lattice system retain and emphasize significantly more of the relevant image detail than do the fingerprints synthesized by the standard algorithm.

Inquiries can be addressed to:
Alex Sherstinsky (e-mail: shers@media.mit.edu) or to
Rosalind W. Picard (e-mail: picard@media.mit.edu),
MIT Media Laboratory, E15-383, 20 Ames Street, Cambridge, MA 02139.

1 Introduction

The present research has originated in the investigation of the usefulness of reaction-diffusion systems for modeling natural textures. A reaction-diffusion system is a set of heat equations, coupled by, typically non-linear, reaction terms. The reaction-diffusion model was first proposed by Turing in 1952 in order to explain coating mammalian patterns, such as, for example, zebra stripes, leopard spots, *etc.*, and, until recently, reaction-diffusion systems have been researched predominantly by mathematical biologists working on theories of natural pattern formation and by chemists working on modeling the dynamics of complex chemical reactions [1], [2], [3], [4], [5], [6], [7], [8], [9], [10], [11]. However, the past three years have seen a significant surge in interest in reaction-diffusion systems, primarily for exploiting them in the areas of computer graphics and image processing. The graphics community's interest in reaction-diffusion systems stems from their ability to model and synthesize directly on a three-dimensional object a wide class of natural textures [12], [13]. In the realm of image processing, reaction-diffusion systems have shown promise for texture segmentation and classification [14].

In order to possess pattern formation properties, a reaction-diffusion system must exhibit local instability to small non-homogeneous perturbations. In addition, practical considerations dictate that the system's state variables should be bounded in the large-signal regime. A major difficulty associated with the reaction-diffusion system paradigm in its standard form is that the system possesses this property only for a restricted class of non-linear reaction functions. This drawback narrows the scope of the model's engineering applications.

A common approach aimed at preventing numerical overflow from plaguing the simulations of reaction-diffusion systems on the digital computer has been to clip the magnitudes of the state variables by adding an "if" statement to the numerical method (*e.g.*, Forward Euler) used for solving the system of differential equations [13]. For some reaction-diffusion systems, this technique eventually manages to stop the state variables from changing between successive time steps. However, it does not guarantee that the system will reach equilibrium, even if the values of the state variables are artificially kept from changing. Moreover, controlling a system of differential equations from within the numerical method destroys the mathematical integrity of the original dynamical system.

The main contribution of this paper is the formulation of the clipped M-lattice system as a more practical and flexible extension of the reaction-diffusion model [15], [16]. By using a warping function to facilitate boundedness, this new system allows more flexible non-linear interactions than the reaction-diffusion system. Furthermore, in contrast with the original reaction-diffusion system, convergence of the clipped M-lattice system to a fixed point has been observed in computer simulation for a large variety of non-linear reaction functions. In order to account for some of these observations, we have proven the total stability of a subclass of the clipped M-lattice system [17]. The M-lattice system is closely related to the analog Hopfield network [18], [19], [20], [21] and the cellular neural network [22], [23], [24], [25], but has more flexibility in how its variables interact. The model's ability to inherit the pattern-formation aspects of reaction-diffusion systems is illustrated in an application to the restoration and enhancement of scanned fingerprint images.

The rest of this document is organized as follows. Section 2 summarizes the basic properties of the reaction-diffusion model. Then Section 3 reviews the M-lattice system. Following that, Section 4 derives the pattern-formation properties of one type of the clipped M-lattice system and applies it to the pre-processing of fingerprints. Finally, Section 5 summarizes the report.

2 Reaction-Diffusion System

Turing's paper titled "The Chemical Basis of Morphogenesis" was a first attempt to provide a scientific explanation for the patterns of pigmentation in animals [1]. Many mammals have prominent coat markings. For example, zebras have stripes, giraffes have contoured patches, leopards and cheetahs have spots; the furs of many dogs and cats also display various forms of stripes and patches of different color. In addition, many tropical fish exhibit colorful patterns of spots and stripes.

Turing proposed to model nature's behavior by an interaction of chemicals that he called "morphogens". The simplest model uses two morphogens: the "activator" and the "inhibitor". The morphogens themselves are produced by chemical reactions among particular enzymes in every cell of the animal's skin during the animal's embryonic stages [11].

According to this model, the two morphogens react with each other; however, the model consisting of reaction alone cannot account for the tremendous variety of coating patterns observed in animals. Since there is no inter-cellular flow of morphogens in the model, every cell acts as an independent autonomous system, producing the final morphogen concentrations based only on random initial concentrations. Therefore, cells end up in stable states that have no correlation or spatial structure, unlike the majority of patterns occurring in nature. In order to supplement the model with the needed transport mechanism, Turing encorporated a diffusion term into the system of equations.

As a case study, Turing modeled the tentacle formation in hydra (a small tubular fresh-water polyp) with

a 1-D reaction-diffusion system:

$$\begin{aligned}
\frac{\partial \psi_A(x,\ t)}{\partial t} &= \psi_A(x,\ t)\cdot\psi_I(x,\ t) - \psi_A(x,\ t) - 12 \\
&+ q(x) + D_A\frac{\partial^2\psi_A(x,\ t)}{\partial x^2}, \\
\frac{\partial \psi_I(x,\ t)}{\partial t} &= 16 - \psi_A(x,\ t)\cdot\psi_I(x,\ t) \\
&+ D_I\frac{\partial^2\psi_I(x,\ t)}{\partial x^2}, \qquad (1)
\end{aligned}$$

where $q(x)$, called the "evocator", is a waveform of small random perturbations, and D_A and D_I are the diffusion rates of the activator and the inhibitor morphogens, respectively.

To gain a qualitative understanding of the operation of a two-morphogen reaction-diffusion system, consider two morphogens, the activator and the inhibitor, each reacting with itself and the other. While the reactions influence local concentrations of the two morphogens, the diffusion transports the morphogens from cell to cell. Suppose the activator is auto-catalytic but diffuses slowly. In other words, its concentration increases in proportion to the amount already present, but its diffusion rate is low compared to that of the inhibitor. Thus the activator and the inhibitor create two opposing tendencies. On one hand, the activator concentration grows at a high rate locally, but does not spread fast enough to replace the inhibitor everywhere. On the other hand, the inhibitor consumes the activator at a low rate locally, but, because of its high diffusion constant, the inhibitor is delivered faster to remote sites, keeping the activator concentration finite everywhere. The competition between these two tendencies causes the concentration profiles of the activator and the inhibitor to settle into patterns of peaks and valleys.

We now summarize Turing's analysis. The cells of hydra are assumed to be equally spaced and comprise a periodic 1-D lattice with the period of N_x cells. Using a popular discretization of the second derivative [26], turns (1) into:

$$\begin{aligned}
\frac{\partial \psi_A(n_x,\ t)}{\partial t} &= \psi_A(n_x,\ t)\cdot\psi_I(n_x,\ t) - \psi_A(n_x,\ t) \\
&- 12 + q(n_x) + D_A[\psi_A(n_x+1,\ t) \\
&- 2\psi_A(n_x,\ t) + \psi_A(n_x-1,\ t)], \\
\frac{\partial \psi_I(n_x,\ t)}{\partial t} &= 16 - \psi_A(n_x,\ t)\cdot\psi_I(n_x,\ t) \\
&+ D_I[\psi_I(n_x+1,\ t) - 2\psi_I(n_x,\ t) \\
&+ \psi_I(n_x-1,\ t)], \\
\psi_A(n_x+N_x,\ t) &= \psi_A(n_x,\ t), \\
\psi_I(n_x+N_x,\ t) &= \psi_I(n_x,\ t). \qquad (2)
\end{aligned}$$

Linearization around a fixed point is commonly the first step in analyzing a non-linear dynamical system. The "small-signal" reaction-diffusion system corresponding to (2) is:

$$\begin{aligned}
\frac{\partial \psi_{A,s}(n_x,\ t)}{\partial t} &= 3\psi_{A,s}(n_x,\ t) + 4\psi_{I,s}(n_x,\ t) \\
&+ D_A[\psi_{A,s}(n_x+1,\ t) - 2\psi_{A,s}(n_x,\ t) \\
&+ \psi_{A,s}(n_x-1,\ t)], \\
\frac{\partial \psi_{I,s}(n_x,\ t)}{\partial t} &= -4\psi_{A,s}(n_x,\ t) - 4\psi_{I,s}(n_x,\ t) \\
&+ D_I[\psi_{I,s}(n_x+1,\ t) - 2\psi_{I,s}(n_x,\ t) \\
&+ \psi_I(n_x-1,\ t)], \\
\psi_{A,s}(n_x+N_x,\ t) &= \psi_{A,s}(n_x,\ t), \\
\psi_{I,s}(n_x+N_x,\ t) &= \psi_{I,s}(n_x,\ t), \qquad (3)
\end{aligned}$$

where the subscript "s"denotes a small deviation from the equilibrium value:

$$\psi_{A,eq}(n_x,\ t=t_0) = \psi_{I,eq}(n_x,\ t=t_0) = 4.$$

The combination of discretization and linearization has turned spatial derivatives into spatial convolutions, making the variables corresponding to different spatial indices in (3) intermixed. Variables are separated in a standard way by applying the Discrete Fourier Transform (DFT), turning convolutions into multiplications:

$$\begin{aligned}
\frac{\partial \psi_{A,s}(k_x,\ t)}{\partial t} &= 3\psi_{A,s}(k_x,\ t) + 4\psi_{I,s}(k_x,\ t) \\
&- 4D_A\psi_{A,s}(k_x,\ t)\sin^2\left(\frac{\pi k_x}{N_x}\right), \\
\frac{\partial \psi_{I,s}(k_x,\ t)}{\partial t} &= -4\psi_{A,s}(k_x,\ t) - 4\psi_{I,s}(k_x,\ t) \\
&- 4D_I\psi_{I,s}(k_x,\ t)\sin^2\left(\frac{\pi k_x}{N_x}\right), \\
\psi_{A,s}(k_x+N_x,\ t) &= \psi_{A,s}(k_x,\ t), \\
\psi_{I,s}(k_x+N_x,\ t) &= \psi_{I,s}(k_x,\ t). \qquad (4)
\end{aligned}$$

The equations in (4) are a special case of the two-morphogen linear reaction-diffusion system of the form:

$$\begin{aligned}
\frac{\partial \psi_{A,s}(k_x,\ t)}{\partial t} &= \psi_{A,s}(k_x,\ t)\left[r_{11} - 4D_A\sin^2\left(\frac{\pi k_x}{N_x}\right)\right] \\
&+ r_{12}\psi_{I,s}(k_x,\ t), \\
\frac{\partial \psi_{I,s}(k_x,\ t)}{\partial t} &= \psi_{I,s}(k_x,\ t)\left[r_{22} - 4D_I\sin^2\left(\frac{\pi k_x}{N_x}\right)\right] \\
&+ r_{21}\psi_{A,s}(k_x,\ t), \qquad (5)
\end{aligned}$$

where the diffusion rates, D_A and D_I, are restricted to be non-negative. The constants $r_{m_1m_2}$ are called the marginal reaction rates.

Depending on the eigenvalues and the initial conditions, the system (5) can exhibit six types of solutions:

- $\lambda_1(k_x)$ and $\lambda_2(k_x)$ are a complex pair with a negative real part $\Longrightarrow$ decaying traveling waves;
- $\lambda_1(k_x)$ and $\lambda_2(k_x)$ are a complex pair with a positive real part $\Longrightarrow$ growing traveling waves;

- two identical decaying traveling waves moving in the opposite directions $\Longrightarrow$ decaying standing waves;
- two identical growing traveling waves moving in the opposite directions $\Longrightarrow$ growing standing waves;
- both $\lambda_1(k_x)$ and $\lambda_2(k_x)$ are real and negative $\Longrightarrow$ decaying spatially-stationary waves; and
- either $\lambda(k_x)$ is real and positive $\Longrightarrow$ growing spatially-stationary waves.

The solution is a non-stationary spatial wave, unless $\lambda(k_x)$ is real. Both traveling wave and standing wave solutions are called non-stationary, because the amplitudes of such waves undergo sign changes. Table 1 summarizes all the possibilities for a 2×2 reaction-diffusion system.

Traveling waves cannot model an animal coat texture, because they do not produce a constant spatial pattern. Also, if the real part of $\lambda(k_x)$ is negative, then the spatial harmonics decay to zero. Thus, for explaining the formation of natural patterns, such as zebra stripes and leopard spots, it was the last mode that received a lot of attention. The other modes of reaction-diffusion systems have also been used, for instance, in modeling the behavior of oscillating chemical reactions [9], [11].

The only mode of the system in (5) that is capable of producing stationary spatial waves is the one corresponding to $\lambda(k_x) \in \Re$, $\lambda(k_x) > 0$ for some range of k_x. Since the amplitude of every k_x that belongs to this band of spatial frequencies grows as a function of time, the system becomes unstable for that particular spatial frequency. Therefore, in order to produce stationary spatial waves, the system must be unstable for at least one spatial frequency. The harmonic $k_x = 0$ is excluded from the band of unstable wave numbers by definition so as to maintain stable equilibrium levels in the absence of diffusion. Thus, the system should be unaffected by homogeneous perturbations.

Turing has determined the conditions on D_A and D_I, under which the system in (5) is stable to homogeneous (*i.e.*, DC) perturbations and unstable to non-homogeneous (*i.e.*, AC) perturbations at least for one value of k_x [1]. Turing gave the name "chemical wavelength" to this dominant spatial frequency, characteristic of (1).

Intuitively, one often thinks of diffusion as a phenomenon that smoothes temperature and concentration gradients and brings stability. Counter to common intuition, however, reaction-diffusion systems are purposefully set up in such a way that diffusion is necessary in order to cause instability. A possible intuitive explanation for the "diffusional", or "Turing", instability can be stated as follows. Without the diffusion, there is only enough morphogen to sustain a pilot reaction, and then the system is stable. However, when the morphogen concentration is non-homogeneous, the diffusion "squirts in some extra morphogen", which "fuels" the reaction. The morphogen concentration explodes, thereby driving the system unstable.

As the amplitude of the dominant mode grows, the linear analysis ceases to be valid. However, Turing argues that the linear behavior predicts the overall non-linear behavior reasonably well. Subsequent computer simulations have confirmed this for many reaction-diffusion systems [2], [3], [9], [11], [17].

The present research emphasizes the use of reaction-diffusion models for synthesis and analysis of textures, regardless of whether or not every detail of the model considered is biologically plausible. Thus it has been shown that when discretized diffusion is replaced by a general FIR filter, even single-morphogen systems become capable of pattern formation [17]. This capability will be utilized in applying the model to fingerprint restoration, which is described in Section 4.

3 M-Lattice System

A vast variety of non-linear reaction functions do not only facilitate local instabilities, essential for synthesizing textures, but also cause undesirable large-signal growth of state variables without bound. In order to alleviate this problem, while retaining the pattern-formation capabilities, we propose to study the reaction-diffusion system on a spatial grid and allow a general FIR filter in place of the discretized diffusion operator. By controlling the growth of the non-linear terms with a sigmoidal warping function, we arrive at the M-lattice system. As we show in Section 4, using a warping function does not destroy the small-signal behavior of the model, which is responsible for the formation of spatial patterns. Moreover, one can design the system such that the morphogen concentrations are bounded in the large-signal regime. The origin of the name "M-lattice system" comes from its roots in the reaction-diffusion paradigm, where M stands for the number of morphogens, or layers, in the lattice.

3.1 General Definition

Let $\psi_i(t) \in \Re$ be a state variable as a function of time at each lattice point i, where $i = 1, \ldots, N$. Let $\chi_i(t)$ be an output variable, obtained from $\psi_i(t)$ via $\chi_i(t) = g(\psi_i(t))$. The "warping" function, $g(u)$, an example of which appears in Figure 1, must be of a saturating type so as to limit the range of the output variables. Construct $\vec{\psi}(t)$ and $\vec{\chi}(t)$ by concatenating $\psi_1(t), \ldots, \psi_N(t)$ and $\chi_1(t), \ldots, \chi_N(t)$, respectively into column vectors.

Definition 3.1 *Suppose that the given functions, $f_i(\vec{\chi}(t))$, are continuous, differentiable, and bounded. Let the matrix* **A** *be real with all eigenvalues having*

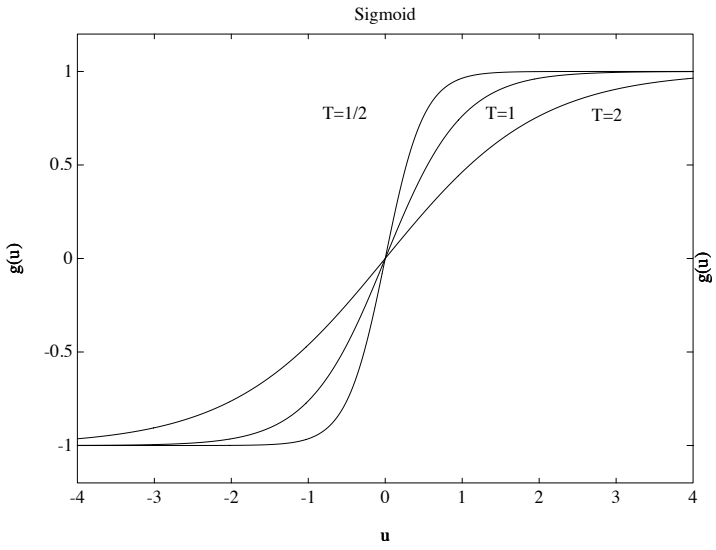

Figure 1: Plots of a sigmoidal warping function for three different temperatures.

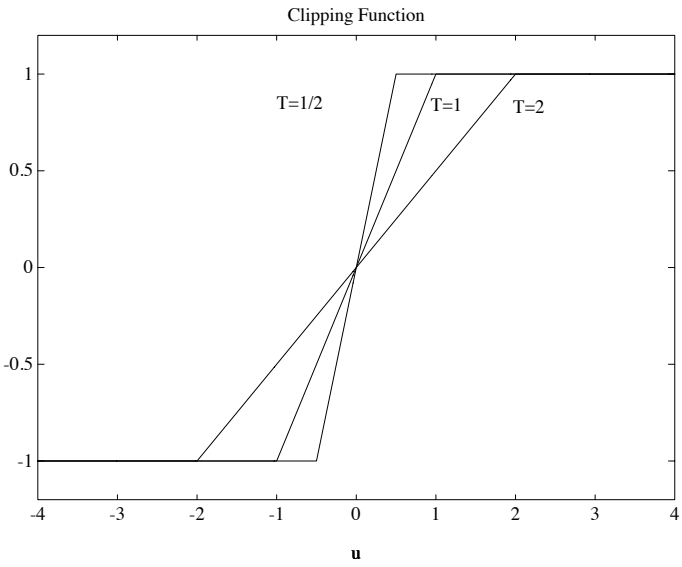

Figure 2: Plots of the clipping warping function for three different temperatures.

negative real parts: $\mathbf{A} \in \Re^{N \times N}$, $\mathbf{A} = [a_{ij}]$, *and* $\forall\ i\ \Re(\lambda_i[\mathbf{A}]) < 0$. *Define* $\vec{f}(\vec{\chi}(t))$ *by concatenating* $f_1(\vec{\chi}(t))$, ..., $f_N(\vec{\chi}(t))$ *into a column vector. Then the* M*-lattice system is a possibly non-linear autonomous dynamical system, described by the following equation:*

$$\frac{d\vec{\psi}(t)}{dt} = \mathbf{A}\vec{\psi}(t) + \vec{f}(\vec{\chi}(t)). \tag{6}$$

A crucial property of the M-lattice system is that its state variables are bounded [17].

3.2 Clipped M-Lattice System

Consider the M-lattice system, (6), in which $\vec{f}(\vec{\chi}(t)) \stackrel{\text{def}}{=} \vec{\nabla}_{\vec{\chi}}\Phi(\vec{\chi}(t))$ and $g(u)$ is the following "clipping" function:

$$\left.\begin{array}{rcl} \dfrac{dg(u)}{du} & = & \left\{ \begin{array}{ll} \dfrac{1}{T}, & |u| < T; \\ 0, & |u| \geq T. \end{array} \right. \\ g(u) & = & \dfrac{1}{2}\left(\left| \dfrac{u}{T} + 1 \right| - \left| \dfrac{u}{T} - 1 \right| \right); \quad T \in \Re_+. \end{array} \right\} \tag{7}$$

This function is plotted in Figure 2.

Definition 3.2 *Suppose that the given function,* $\Phi(\vec{\chi}(t))$*, is continuous, twice-differentiable, and bounded. Let the matrix* $\mathbf{A}$ *be real, symmetric, and negative-definite:* $\mathbf{A} \in \Re^{N \times N}$, $\mathbf{A} = [a_{ij}]$, $\mathbf{A} = \mathbf{A}^T$, *and* $\forall\ i\ \lambda_i[\mathbf{A}] < 0$. *Then the clipped* M*-lattice system is the following possibly non-linear dynamical system:*

$$\frac{d\vec{\psi}(t)}{dt} = \mathbf{A}\vec{\psi}(t) + \vec{\nabla}_{\vec{\chi}}\Phi(\vec{\chi}(t)). \tag{8}$$

As part of the analysis, we have shown that a subclass of the clipped M-lattice system possesses total stability, which is manifested in asymptotic convergence, regardless of the initial conditions [17].

Proposition 3.1 *Consider a special case of the* M*-lattice system, (8), in which* $\mathbf{A} = Diag\ \{a_1, \ldots, a_N\}$, $\forall\ i\ a_i < 0$. *Any solution trajectory of this diagonal-state clipped* M*-lattice system converges to a finite asymptotically stable fixed point,* $\vec{\psi} \in \Re^N$ *(or* $\vec{\chi} \in [-1,\ 1]^N$*).*

Thus far, no proof of total stability exists for the more general system, (8). However, fixed points of the form $\vec{\chi} \in \{-1,\ 1\}^N$ are asymptotically stable [17]. In all experiments of the type that we discuss below, the general clipped M-lattice system exhibited convergence in computer simulation.

3.3 Comparison to Other Models

Several key aspects of the general M-lattice system, (6), with various saturating warping functions are unique when compared to other closely related models. Unlike the analog Hopfield network or the cellular neural network, the M-lattice system allows the $\mathbf{A}$ matrix to have off-diagonal elements. In addition, the interactions among the output variables, $\chi_i(t)$ can in principle be prescribed by a very general non-linear function, $\vec{f}(\vec{\chi}(t))$. This flexibility enables the M-lattice system to capture the behavior of a wider variety of physical systems.

If $\mathbf{A}$ is a diagonal matrix with negative elements on the main diagonal and $\Phi(\vec{\chi}(t))$ is a multilinear polynomial (*i.e.*, a polynomial whose independent variables

have the powers zero or one [21]), then the M-lattice system with a sigmoidal warping function becomes the analog Hopfield network. For binary outputs, the M-lattice system, similarly to the analog Hopfield network, is capable of optimization in the sense of the Hamming distance of one [21], [17].

If $\mathbf{A}$ is a diagonal matrix with the same negative element on the main diagonal and $\vec{\nabla}_{\vec{\chi}}\Phi(\vec{\chi}(t))$ is a circulant (or block-circulant) symmetric matrix, which represents the convolution with a linear shift-invariant FIR filter, then the clipped M-lattice system, (8), becomes the original cellular neural network [22], [23], [24], [25].

4 Restoration And Halftoning Of Fingerprints Using M-Lattice System

A typical fingerprint identification system contains a pre-processing step, which involves the halftoning of the original scanned and finely quantized fingerprint image. The essential steps comprising the identification sequence are: determining the type of the fingerprint, counting of ridges and bifurcations, and locating the core. A binary fingerprint image is more amenable for these tasks than a gray-scale fingerprint image [27].

We propose a pre-processing scheme that not only halftones the original fingerprint image, but also removes artifacts that can hinder the identification process. The method uses the ability of the clipped M-lattice system to excite locally-growing stationary spatial waves, which are the signature of reaction-diffusion systems, as well as to produce equilibrium images that have binary-valued pixels.

The motivation for using the reaction-diffusion aspect of the clipped M-lattice system is that fingerprint images have distinct patterns of thin curves, remotely resembling zebra stripes. Reinforcing the harmonics that create these curves will emphasize the essentials of the fingerprint, while suppressing the artifacts.

As mentioned in Section 3, halftoned images that are fixed points of the clipped M-lattice system are asymptotically stable. This means that even though reaction-diffusion is a small-signal phenomenon, the large-signal evolution of the system toward a binary output image does not destroy the restoration performed by the linear behavior.

Let $\mathbf{A}$ and $\mathbf{H}$ be block-circulant symmetric matrices. Then the clipped M-lattice system, (8), can be written as follows:

$$\frac{d\psi(\vec{n},\ t)}{dt} \quad = \quad a(\vec{n}) * \psi(\vec{n},\ t) + s(\vec{n}) - h(\vec{n}) * \chi(\vec{n},\ t), \quad (9)$$

where $\vec{n} \in \mathcal{Z}^2$, $a(\vec{n})$ and $h(\vec{n})$ are the FIR filters, corresponding to $\mathbf{A}$ and $\mathbf{H}$, respectively, and $s(\vec{n}) \in [-1,\ 1]$ is the original finely quantized input image signal.

The advantage of using this type of the clipped M-lattice system for the pre-processing of fingerprints is that it can be guaranteed to produce binary outputs [17].

Proposition 4.1 *Assume that the clipped M-lattice system, (8), is totally stable. Suppose that $\mathbf{A}$ and $\mathbf{H}$ used in the clipped M-lattice system, (8), correspond to symmetric filters, and the following conditions are satisfied:*

$$\begin{cases} a(\vec{0}) + \dfrac{h(\vec{0})}{T} - \displaystyle\sum_{\vec{n}\neq\vec{0}} |a(\vec{n})| \\ \qquad > \quad a(\vec{0}) + \left| a(\vec{k}) + \dfrac{h(\vec{k})}{T} \right| + \displaystyle\sum_{\vec{n}\neq\vec{0},\vec{n}\neq\vec{k}} |a(\vec{n})|, \\ a(\vec{0}) + \dfrac{h(\vec{0})}{T} - \displaystyle\sum_{\vec{n}\neq\vec{0}} |a(\vec{n})| \ > \ 0, \\ \quad \textit{where } \vec{k} \ = \ \arg\max\limits_{\vec{n}\neq\vec{0}} \left| a(\vec{n}) + \dfrac{h(\vec{n})}{T} \right|. \end{cases}$$

Then $\vec{\chi} \in \{-1,\ 1\}^N$.

It now remains to demonstrate that (9) possesses the desired pattern-formation properties.

4.1 Small-Signal Regime: Reaction-Diffusion

Choose $\mathbf{A}$ and $\mathbf{H}$ such that the unique interior fixed point, $\psi(\vec{n}) \in (-1,\ 1)$, of (9) is at $s(\vec{n})$. Denote the DFT representations of the filters by $A(\vec{k})$ and $H(\vec{k})$. Then all the $A(\vec{k})$ coefficients must be negative [26]. Before $\psi(\vec{n},\ t)$ reaches the clipping levels of (7), (9) simplifies to:

$$\frac{d\psi(\vec{n},\ t)}{dt} \quad = \quad s(\vec{n}) + \left(a(\vec{n}) - \frac{1}{T} h(\vec{n}) \right) * \psi(\vec{n},\ t). \quad (10)$$

Taking the DFT of both sides of (10) in order to separate variables yields:

$$\frac{d\psi(\vec{k},\ t)}{dt} \quad = \quad S(\vec{k}) + \left(A(\vec{k}) - \frac{1}{T} H(\vec{k}) \right) \psi(\vec{k},\ t), \quad (11)$$

whose solution for each $\vec{k}$ is:

$$\psi(\vec{k},\ t) \quad = \quad \left[S(\vec{k}) + \frac{S(\vec{k})}{F(\vec{k})} \right] \exp\left\{ F(\vec{k}) t \right\} - \frac{S(\vec{k})}{F(\vec{k})}, \quad (12)$$

where $F(\vec{k}) \stackrel{\text{def}}{=} A(\vec{k}) - \dfrac{1}{T} H(\vec{k})$, and the initial condition is set to $S(\vec{k})$, the DFT equivalent of the original image. Hence, from the discussion in Section 2, making $F(\vec{k})$ positive for a set of spatial frequencies creates the onset of growing spatially-stationary waves.

The adaptive filter, $H(\vec{k})$, was designed so as to include the information about the dominant orientation at each pixel of the original image, shown in Figure 3(a) [28]. The dominant orientation at a pixel is characterized by the angle, $\theta_i \in [-\pi,\ \pi]$, and by the relative strength (or magnitude), $m_i \in [0,\ 1]$, of that angle's presence at pixel i. Each filter is a 2-D Gaussian, whose level sets are oriented ellipses. Denote the diagonal matrix of variances by $\mathbf{V}_i$, the rotation matrix by $\mathbf{\Theta}_i$, and the position vector by $\vec{n} \in \mathcal{Z}^2$:

$$\mathbf{V}_i = \begin{bmatrix} \sigma_{i,x}^2 & 0 \\ 0 & \sigma_{i,y}^2 \end{bmatrix}, \mathbf{\Theta}_i = \begin{bmatrix} \cos\theta_i & -\sin\theta_i \\ \sin\theta_i & \cos\theta_i \end{bmatrix}. \quad (13)$$

The relative sizes of $\sigma_{i,x}^2$ and $\sigma_{i,y}^2$ depend on m_i and determine the skewness of filters with respect to the dominant orientation:

$$\sigma_{i,y}^2 = \frac{L}{2}(1 - m_i), \quad \sigma_{i,x}^2 = L - \sigma_{i,y}^2, \quad (14)$$

where $L \times L$ is the size of the filter mask in pixels. Then the (unnormalized) oriented low-pass filter is given by:

$$h_i(\vec{n}) \quad = \quad \exp\left\{-\vec{n}^T \mathbf{\Theta}_i^T \mathbf{V}_i \mathbf{\Theta}_i \vec{n}\right\}. \quad (15)$$

Pertinent to fingerprint restoration is the kind of filtering that delineates the ridges, while cancelling fluctuations in the DC level and getting rid of extraneous information. Thus, $H(\vec{k})$ and $A(\vec{k})$ are constructed in a way that makes the frequency bands corresponding to the ridges have negative DFT coefficients, and the $\frac{1}{T}$ factor amplifies the effect.

4.2 Large-Signal Regime: Halftoning

Proposition 4.1 gives sufficient conditions for ensuring that the large-signal equilibrium output pattern is binary. These conditions place restrictions on the elements of the filter $h(\vec{n})$. The needed additional flexibility is provided by the $A(\vec{k})$ filter, which has negative DFT coefficients. For instance, in fingerprint restoration, we use $A(\vec{k})$ to cancel the unwanted harmonics, most importantly the DC term, $\vec{k} = \vec{0}$.

Figure 3(a) is a typical scanned and finely quantized fingerprint image from the NIST database. The original image is 512×512 pixels and was low-pass filtered and down-sampled by a factor of 2 in each dimension in order to speed up the computation. From the figure, it can be seen that the original fingerprint is corrupted by a number of scratches, and several regions are obscured by uneven illumination. As shown in Figure 3(b), the standard fingerprint halftoning method, based on adaptive median filtering and thresholding, only makes these artifacts more apparent, because it increases the image's contrast [29]. The adaptive threshold is set to the average of the minimum and the maximum gray levels within some neighborhood surrounding each pixel of the original fingerprint image. The optimal size of the window was determined to be 5×5 pixels by trial and error. Other standard halftoning methods, such as ordered dither or error diffusion, will perform poorly also, because they have no built-in restoration mechanism and will halftone both signal and noise alike.

Using a two-stage system, consisting of some conventional image restoration algorithm, followed by adaptive-thresholding type of halftoning is another viable alternative. However, there are two arguments in favor of using the clipped M-lattice system-based approach. First, the analysis of Section 4.1 implies that the attainable signal-to-noise ratios can be very large. Essentially, the clipped M-lattice system applies the filters, $a(\vec{n})$ and $h(\vec{n})$, an infinite number of times by the virtue of being a continuous-time system. Second, no separate halftoning step is needed, since the clipped M-lattice system binarizes the image by setting the elements of $h(\vec{n})$ in accordance with Proposition 4.1.

Other researchers have succeeded in using the reaction-diffusion paradigm for performing operations that are relevant to the pre-processing of fingerprint images. One effort, which, incidentally, was not specifically targeted for fingerprint restoration, deals with replacing portions of fingerprints with patches, whose visual appearance resembles that of a generic fingerprint texture [30], [31]. However, the inserted patch may turn out to be substantially dissimilar from the missing section of the original image. Another report describes the restoration of noisy fingerprints with a particular reaction-diffusion system [32]. However, the output image is not a halftone. Our new technique is inspired by these previous approaches and accomplishes restoration and halftoning simultaneously.

Figure 3(c) displays the processed fingerprint image. The scratches have been removed and the unevennesses in the DC levels throughout the image have been eliminated. Essential detail such as ridges and bifurcations appear as continuous black curves, distinctly enhanced against a noise-free white background. Moreover, ridges and bifurcations have been extended even into the regions where they are barely detectable in the original image. This illustrates the celebrated synergetic property of reaction-diffusion systems: the emergence from noise of a spatial pattern, whose qualitative characteristics are pre-determined by the system's parameters [1], [11]. Using the connection machine (CM-2), the final image is produced in 25 iterations at the time step of 0.1 sec. For viewing convenience, Figure 4 shows a 128×128 pixel middle-top section of each respective image of Figure 3, magnified by a factor of 2 in both dimensions.

class of wave	both $\Re[\lambda] < 0$ (stable)	either $\Re[\lambda] \geq 0$ (unstable)	λ	type of solution
traveling	decaying	growing	complex	oscillatory
standing	decaying (sum of a decaying traveling wave and its reflection)	growing (sum of a growing traveling wave and its reflection)	complex	oscillatory
stationary	decaying	growing	real	non-oscillatory

Table 1: The kinds of modes admitted by a 2×2 reaction-diffusion system. The terms "decaying" and "growing" refer to the temporal behavior.

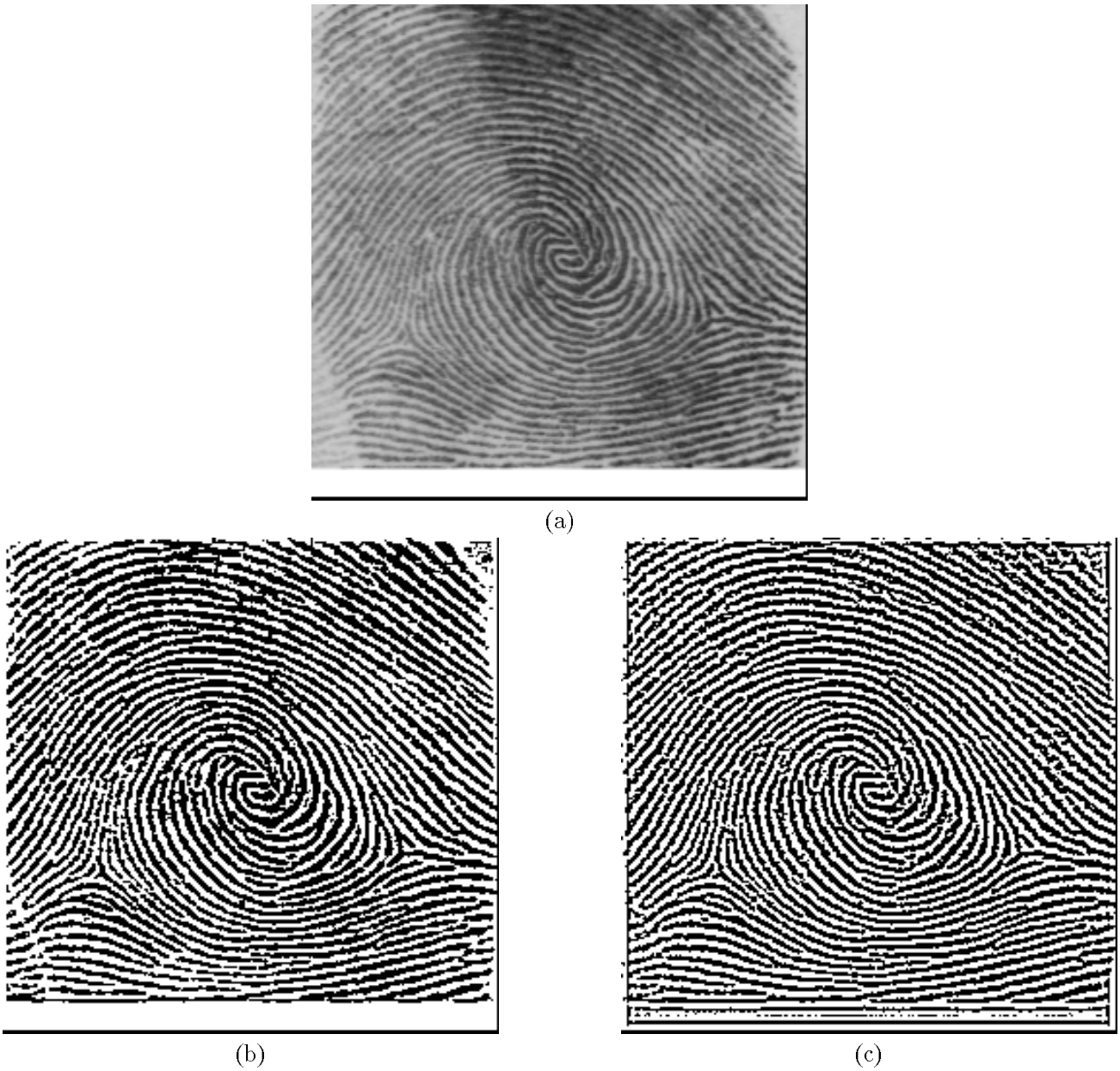

(a)

(b)

(c)

Figure 3: Restoration and halftoning of fingerprints. (a) the original "fingerprint" image; (b) the "fingerprint" image halftoned by a standard adaptive-threshold method; (c) the "fingerprint" image restored and halftoned by the clipped M-lattice system operating in the reaction-diffusion mode utilizing orientation information at each pixel of the original.

(a)

(b)

(c)

Figure 4: Magnification of a 128×128 pixel middle-top section of the images in Figure 3. (a) original; (b) halftoned by a standard adaptive-threshold method; (c) restored and halftoned by the clipped M-lattice system.

5 Conclusions

We have reviewed the reaction-diffusion model with emphasis on its pattern-formation potential. In an attempt to broaden the class of non-linear reaction functions that lead to bounded reaction-diffusion systems, we have introduced the M-lattice system, a massively parallel non-linear dynamical system. We have shown that the clipped M-lattice systems is capable of synthesizing textured images by the same mechanisms as does the reaction-diffusion system.

The problem of fingerprint restoration and halftoning is a natural application of the clipped M-lattice system, because of its ability to synthesize zebra stripes, which appear qualitatively similar to ridges and bifurcations comprising human fingerprints. Using orientation detection for designing the system parameters so as to emphasize the significant features of a fingerprint image causes the clipped M-lattice system to act as an infinitely-aggressive band-pass filter. As a result, ridges and bifurcations are extracted at the highest contrast, even if they are only faintly detectable in the original image, while scratches, unevennesses in illumination, and other extraneous detail are removed. The contrast of the restored features is enhanced with the help of the binarization capability of the clipped M-lattice system.

References

[1] A. M. Turing, "The chemical basis of morphogenesis," *Philosophical Transactions of Royal Society of London*, vol. 237, no. B, pp. 37–72, 1952.

[2] J. B. L. Bard and I. Lauder, "How well does Turing's theory of morphogenesis work?," *Journal of Theoretical Biology*, vol. 45, pp. 501–531, 1974.

[3] J. B. L. Bard, "A model for generating aspects of zebra and other mammalian coat patterns," *Journal of Theoretical Biology*, vol. 93, pp. 363–385, 1981.

[4] H. Meinhardt, *Models Of Biological Pattern Formation*. New York, NY: Academic Press, 1982.

[5] D. A. Young, "A local activator-inhibitor model of vertebrate skin patterns," *Mathematical Biosciences*, vol. 72, pp. 51–58, 1984.

[6] J. D. Murray, "A pre-pattern formation mechanism for animal coat markings," *Journal of Theoretical Biology*, vol. 88, pp. 161–199, 1981.

[7] J. D. Murray, "On pattern formation mechanisms for lepidopteran wing patterns and mammalian coat markings," *Philosophical Transactions of Royal Society of London*, vol. 295, no. B, pp. 473–496, 1981.

[8] J. D. Murray, "Parameter space for Turing instability in reaction diffusion mechanisms: A comparison of models," *Journal of Theoretical Biology*, vol. 98, pp. 143–163, 1982.

[9] N. F. Britton, *Reaction-Diffusion Equations and Their Applications to Biology*. New York, NY: Academic Press, 1986.

[10] J. D. Murray, "How the leopard gets its spots," *Scientific American*, vol. 258, pp. 80–87, Mar. 1988.

[11] J. D. Murray, *Mathematical Biology*. Berlin: Springer-Verlag, 1993.

[12] A. Witkin and M. Kass, "Reaction-diffusion textures," *Computer Graphics*, vol. 25, pp. 299–308, July 1991.

[13] G. Turk, "Generating textures on arbitrary surfaces using reaction-diffusion," *Computer Graphics*, vol. 25, pp. 289–298, July 1991.

[14] C. B. Price, P. Wambacq, and A. Oosterlinck, "Applications of reaction-diffusion equations to image processing," in *Third International Conference on Image Processing and its Applications*, (Warwick, UK), July 1989.

[15] A. Sherstinsky and R. W. Picard, "Reaction-diffusion systems for image processing," in *Proceedings of Workshop on Synergetic Engineering: Applications of Nonlinear Dynamical Systems to Image Processing*, (Sydney, Australia), Apr. 1993.

[16] A. Sherstinsky and R. W. Picard, "M-lattice: A novel non-linear dynamical system and its application to halftoning," in *Proceedings of IEEE International Conference on Acoustics, Speech and Signal Processing (To Appear)*, Apr. 1994.

[17] A. Sherstinsky and R. W. Picard, "M-lattice system: Theory and potential applications," Tech. Rep. (In Preparation), M.I.T. Media Lab Perceptual Computing Group, 1994.

[18] J. J. Hopfield, "Neural networks and physical systems with emergent collective computational abilities," *Proceedings of National Academy of Sciences, USA*, vol. 79, pp. 2554–2558, Apr. 1982.

[19] J. J. Hopfield, "Neurons with graded response have collective computational properties like those of two-state neurons," *Proceedings of National Academy of Sciences, USA*, vol. 81, pp. 3088–3092, May 1984.

[20] J. J. Hopfield and D. W. Tank, ""Neural" computation of decisions in optimization problems," *Biological Cybernetics*, vol. 52, pp. 141–152, 1985.

[21] M. Vidyasagar, "Minimum-seeking properties of analog neural networks with multilinear objective functions," Tech. Rep. (Unpublished), Centre For AI & Robotics, Bangalore, India, 1993.

[22] L. O. Chua and L. Yang, "Cellular neural networks: Theory," *IEEE Transactions on Circuits and Systems*, vol. 35, pp. 1257–1272, Oct. 1988.

[23] L. O. Chua and L. Yang, "Cellular neural networks: Applications," *IEEE Transactions on Circuits and Systems*, vol. 35, pp. 1273–1290, Oct. 1988.

[24] T. Roska and L. O. Chua, "Cellular neural networks with nonlinear and delay-type template elements," in *Proc. IEEE Int. Workshop on Cellular Neural Networks and Applications*, (Budapest, Hungary), 1990.

[25] L. O. Chua and T. Roska, "Stability of a class of nonreciprocal cellular neural networks," *IEEE Transactions on Circuits and Systems*, vol. 37, pp. 1520–1527, Dec. 1990.

[26] G. Strang, *Introduction to Applied Mathematics*. Cambridge, MA: Wellesley-Cambridge Press, 1986.

[27] A. P. Russo, "An automatic system for fingerprint analysis," Master's thesis, Rensselaer Polytechnic Institute, Troy, NY, 1986.

[28] W. T. Freeman and E. H. Adelson, "The design and use of steerable filters," *IEEE Transactions on Pattern Analysis and Machine Intelligence*, vol. PAMI-13, pp. 891–906, Sept. 1991.

[29] "Private communications with Dmitry B. Utyansky, Novintech-Leintec, Ltd.," Feb. 1994.

[30] M. Kass and A. Witkin, "Analyzing oriented patterns," in *Readings In Computational Vision* (M. A. Fischler and O. Firschein, eds.), Morgan Kaufman, 1987.

[31] G. Zorpette, "A horse of a different color," *IEEE Spectrum*, pp. 17–18, July 1992.

[32] C. B. Price, P. Wambacq, and A. Oosterlinck, "Image enhancement and analysis with reaction-diffusion paradigm," *IEE Proceedings*, vol. 137, June 1990.